IEEE Photonics Journal
An IEEE Photonics Society Publication



# A Dual-Frequency Faraday Laser

Volume 12, Number 4, August 2020

Tiantian Shi, *Member, IEEE*
Xiaolei Guan
Pengyuan Chang
Jianxiang Miao
Duo Pan, *Member, IEEE*
Bin Luo, *Member, IEEE*
Hong Guo, *Member, IEEE*
Jingbiao Chen

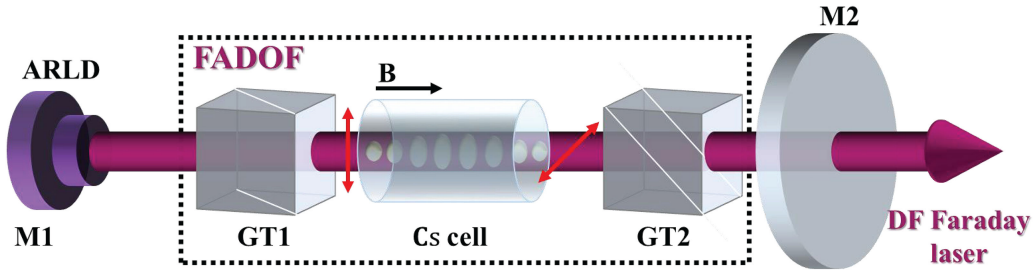


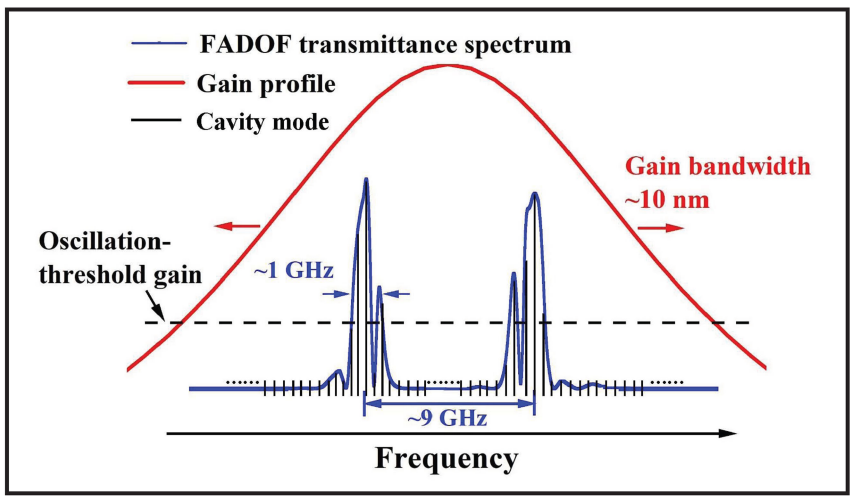


DOI: 10.1109/JPHOT.2020.3006503

# A Dual-Frequency Faraday Laser

**Tiantian Shi**,[1] ***Member, IEEE***, **Xiaolei Guan**,[1] **Pengyuan Chang**,[1] **Jianxiang Miao**,[1] **Duo Pan**,[1] ***Member, IEEE***, **Bin Luo**,[2] ***Member, IEEE***, **Hong Guo**,[1] ***Member, IEEE***, **and Jingbiao Chen** [1]

[1]State Key Laboratory of Advanced Optical Communication Systems and Networks, Institute of Quantum Electronics, Department of Electronics,Peking University, Beijing 100871, China
[2]Beijing University of Posts and Telecommunications, Beijing 100876, China

*DOI:10.1109/JPHOT.2020.3006503*


Manuscript received June 17, 2020; accepted June 29, 2020. Date of publication July 2, 2020; date of current version July 16, 2020. This work was supported by the National Natural Science Foundation of China, NSFC Award 91436210. Corresponding authors: Duo Pan and Bin Luo (e-mail: panduo@pku.edu.cn; luobin@bupt.edu.cn).

**Abstract:** The Faraday laser, with Faraday anomalous dispersion optical filter (FADOF) as frequency-selection element, is a natural narrow-bandwidth light source for laser physic experiments. In this work, a dual-frequency (DF) Faraday laser is demonstrated for the first time on Cs D2 line at 852 nm. The frequencies of the two modes of DF Faraday laser hinge on the peak transition frequencies of 852 nm FADOF transmittance spectrum corresponding to the ground state $F = 4$ and $F = 3$. The frequency difference between the two modes is tunable over a range of 1.4 GHz with the temperature of Cs vapor cell inside the FADOF. The linewidth of each laser mode is less than 33 kHz. Furthermore, the most probable linewidth of the beat-note spectra between the two modes is 902.95 Hz at different vapor-cell temperatures. Such a DF Faraday laser has many potential applications in atomic physics, such as sub-Doppler spectroscopy and coherent population trapping atomic clocks.

**Index Terms:** Faraday anomalous dispersion optical filter (FADOF), diode laser, faraday laser, dual-frequency laser.

## 1. Introduction

Faraday anomalous dispersion optical filter (FADOF) [1], [2], with superiorities of high noise rejection, narrow bandwidth [3], [4], and high transmission, has been detailedly studied in theory and experiment based on different atomic species, such as Na [5], Rb [6], K [7], [8] and Cs [9], [10], for over 60 years [11]. Utilizing the anomalous Faraday effect [9], only the signal with frequency near atomic resonance can be transmitted. Therefore, the FADOF is an excellent filter to distinguish the useful signal from background noise, which is widely applied in optical communication [9], atmospheric lidar [12], [13], and frequency stabilization of diode laser [14]–[16].

The Faraday laser [17]–[19], which is composed of an antireflection-coated laser diode (ARLD) as gain medium, a FADOF as frequency-selection element, and a high-reflectivity mirror for optical feedback, can stably operate at atomic Doppler broadened line with frequency being immune to the current and temperature fluctuation of laser diode (LD). It has been confirmed that the wavelength fluctuation of Faraday laser can achieve no more than $\pm 2$ pm within 48 hours [20]. Compared with the typical external-cavity diode lasers (ECDLs) utilizing interference filters (IFs) [21], [22], gratings [23], [24], or Fabry-Pérot etalons [25], [26] as mode-selection elements, the Faraday lasers

take advantage of the narrow-bandwidth atomic filter for frequency selection with frequency being set by the peak transmission frequency of FADOF. Both the short-term and the long-term frequency stabilities of Faraday laser are demonstrated to be less than its corresponding atomic natural linewidth [18]. With exceptional frequency stability and robustness, the Faraday laser provides quite promising applications in atomic physics.

Previous researches on Faraday lasers exclusively focused on the single-frequency operation [16], [18], [20]. However, the dual-frequency (DF) laser is of great importance in the fields like frequency stabilization and high-resolution spectroscopy. For instance, the locking of frequency difference between two oscillation modes of He-Ne laser in microwave domain is used to stabilize the cavity length, and further optimize the frequency stability of the two-mode He-Ne laser in optical domain [27]. Moreover, the DF Tm:YAG laser, with etalon as intracavity mode-selection element, its frequency difference between the two modes is tunable over several GHz with laser linewidth being smaller than 1 MHz, is a favorable tool for precision spectroscopy experiments [28]. Furthermore, the DF laser can effectively realize high-contrast strongly enhanced absorption spikes in saturation absorption spectroscopy (SAS), which has optimized the fractional frequency stability of the diode laser by about one order of magnitude [29].

In this work, we demonstrate a frequency-tunable DF Faraday laser operating on the Cs D2 line. The frequencies $f_1$ and $f_2$ of the two modes $L_1$ and $L_2$ of DF Faraday laser are mainly depend on the two cavity modes closest to the peak transmission frequencies of FADOF transmittance spectrum corresponding to $6^2S_{1/2}(F=4) \rightarrow 6^2P_{3/2}$ and $6^2S_{1/2}(F=3) \rightarrow 6^2P_{3/2}$, respectively. The frequency difference between $f_1$ and $f_2$ is adjustable from 8.80 GHz to 7.43 GHz as the vapor-cell temperature changes from 36 °C to 55 °C. The linewidth of each laser mode of DF Faraday laser is demonstrated to be less than 33 kHz. Moreover, the most probable beating linewidth between $L_1$ and $L_2$ is 902.95 Hz at the vapor-cell temperature range of 36–55 °C, which indicates a high coherence between the two modes. Such a DF Faraday laser can be extended to the experiments of Doppler-free spectroscopy utilizing DF laser filed [29], [30], as well as coherent population trapping (CPT) atomic clocks [31], [32].

## 2. Experimental Setup

The experimental setup is implemented in Fig. 1. A homemade 852 nm interference-filter external-cavity diode laser (IF-ECDL), with a mode-hop-free interval of 7 GHz, is frequency stabilized to Cs $6^2S_{1/2}(F=4) \rightarrow 6^2P_{3/2}(F=5)$ transition by SAS and is used as the reference laser. The bottom of Fig. 1 is the working schematic of DF Faraday laser, which mainly consists of a gain medium 852 nm ARLD (RWE-0860-06010-1500-SOT02-0000), a frequency-selection element FADOF, and an external-cavity mirror. The optical cavity of DF Faraday laser is composed of mirrors M1 and M2 spacing 69 cm. M1 is the rear facet of ARLD with reflectivity $R_1$ of 90% at 852 nm, while the front facet is coated with anti-reflectivity at 852 nm to prevent the formation of intracavity mode, and M2 is the external-cavity mirror with reflectivity $R_2$ of 99%. The FADOF is composed of a pair of polarization-orthogonal Glan-Taylor prisms, and a 30 mm-long vapor cell filled with pure Cs atoms with a temperature-control precision of 0.1 °C. The vapor cell is placed in an axial magnetic field formed by two bar permanent magnets. Utilizing the optical feedback of external-cavity mirror, two laser modes are realized simultaneously, and the beat-note signal of the two modes $L_1$ and $L_2$ is detected by the photodiode (PD2, Thorlabs PDA8GS, DC-9.5 GHz). Moreover, to verify the Faraday laser operates in DF mode and measure the linewidth of each mode, the Faraday laser and the reference laser overlap in space for optical heterodyne, and are monitored by PD2.

The cavity finesse of the DF Faraday laser can be expressed as $F = \frac{\pi\sqrt{R}}{1-R}$, where $R = r_1 r_2 T_t$, $r_1$ and $r_2$ are the reflectivity coefficient of cavity mirrors M1 and M2, which are equal to $r_1 = \sqrt{R_1} = 0.95$ and $r_2 = \sqrt{R_2} = 0.99$, respectively. The transmissions of Glan-Taylor prisms and Cs vapor cell are 0.70 and 0.80. Therefore, the total transmission is $T_t = 0.56$. The free spectrum range is given by $FSR = c/2L = 217$ MHz, where $c$ is the light speed, and the cavity length $L = 69$ cm. Finally, the resonance bandwidth of the cavity mode of DF Faraday laser is given by $\Delta\nu_c = FSR/F = 44$ MHz.

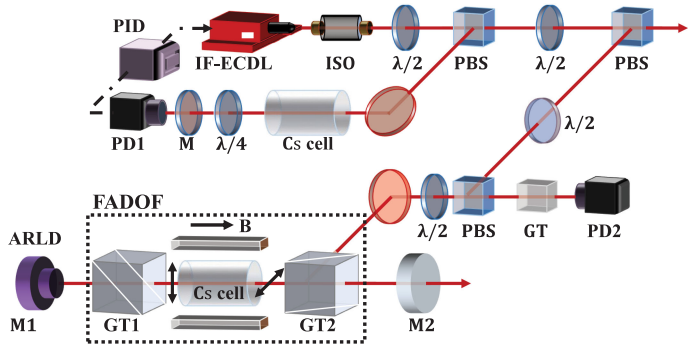


Fig. 1. Experimental setup for DF Faraday laser. The light from 852 nm interference-filter external-cavity diode laser (IF-ECDL) passes through an optical isolator (ISO) and splits on a polarizing beam splitter (PBS). One part double passes through a Cs vapor cell to provide a frequency reference on the photodiode (PD1), and the frequency of IF-ECDL is locked to Cs $6^2S_{1/2}$ F = 4 to $6^2P_{3/2}$ F = 5 hyperfine transition by SAS. The other part coincides with the DF Faraday laser to observe their beat-note spectrum on PD2. The bottom is the working schematic of DF Faraday laser, which consists of a 852 nm antireflection-coated laser diode (ARLD), a Faraday anomalous dispersion optical filter (FADOF), and an external-cavity mirror M2. The rear facet of ARLD is another cavity mirror, which is expressed as M1. The FADOF is composed of a pair of orthogonal Glan-Taylor prisms (GT1 and GT2), a Cs vapor cell, and a pair of bar permanent magnets. The light from DF Faraday laser is exported from GT2 and to be monitored by PD2.

## 3. Results and Discussions

### 3.1 Transmittance Spectrum of FADOF on Cs D2 Line

The light output from 852 nm IF-ECDL is divided into two parts, where one part is stabilized by SAS to provide a frequency reference, and the other, which is different from the scheme in Fig. 1, enters the FADOF in the external cavity of the DF Faraday laser. The SAS and the transmittance spectrum of FADOF on Cs D2 line are displayed in Fig. 2. The top is the Cs 852 nm SAS, whose frequency at $6^2S_{1/2}(F = 4) \rightarrow 6^2P_{3/2}(F' = 5)$ transition is expressed as $f_0$. The bottom is the FADOF transmittance spectrum on Cs D2 line consists of two passbands, which corresponds to $6^2S_{1/2}(F = 4) \rightarrow 6^2P_{3/2}$ and $6^2S_{1/2}(F = 3) \rightarrow 6^2P_{3/2}$ hyperfine lines, respectively, with vapor-cell temperature $T = 43\,^{\circ}$C and axial magnetic filed $B = 330$ G. The peak transmissions of the transmittance spectrum corresponding to $F = 4$ and $F = 3$ are 78% and 72%. The two modes $L_1$ and $L_2$ are separately confined in the two passbands, whose central frequencies $f_1$ and $f_2$ are mainly determined by that of the cavity modes nearest to the peak transmission frequencies of FADOF transmittance spectrum corresponding to F = 4 and F = 3. Limited by the mode-hop-free interval of IF-ECDL, both the SAS and the transmittance spectrum of FADOF are discrete between the two hyperfine levels of Cs ground state.

It is important to note that the light intensity of the laser entering into the FADOF is 5 mW/mm$^2$, which is much stronger than the saturation intensity 1.66 mW/cm$^2$ of Cs D2 line [33]. The pumping effect between hyperfine states becomes dominant since the weak signal light condition is not met [34]. Therefore, the FADOF transmittance spectrum in Fig. 2 is quite different from that calculated by the program ElecSus under weak signal light filtering [35]. However, at present, there is no suitable theoretical model to calculate the FADOF transmittance spectrum under strong light condition. Accordingly, the parameters of FADOF in this work, such as, the vapor-cell temperature and magnetic filed, are based on the experiment.

### 3.2 The Beat-Note Spectrum Between the Reference Laser and the DF Faraday Laser

Under suitable temperature and current of LD, appropriate magnetic field fixed at 330G, combining the optical feedback of cavity mirror M2, the power of DF Faraday laser is around 20 mW. Consequently, the vapor-cell temperature, which is adjustable from 36 °C to 55 °C, is the only variable

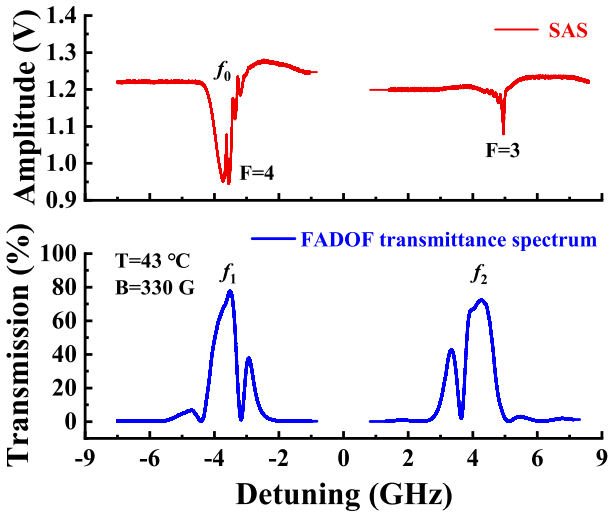


Fig. 2. The SAS (upper) and the transmittance spectrum of FADOF (bottom) on Cs D2 line. Limited by the mode-hop-free interval of 852 nm IF-ECDL, both the SAS and the transmittance spectrum are discrete between the two hyperfine levels of Cs ground state. The left and the right correspond to $6^2S_{1/2}$ $F = 4$ and $F = 3$ to $6^2P_{3/2}$ transition, respectively. The peak transmissions of transmittance spectrum of FADOF are 78% (left) and 72% (right), respectively, with vapor-cell temperature $T = 30\,^{\circ}$C, axial magnetic field $B = 330$ G. The frequency corresponding to $6^2S_{1/2}$ $F = 4$ to $6^2P_{3/2}$ $F' = 5$ transition is expressed as $f_0$, and the frequencies of the two modes from DF Faraday laser are expressed as $f_1$ and $f_2$.

in DF Faraday laser. Under such a condition, the peak transmissions of the FADOF transmittance spectrum corresponding to $6^2S_{1/2}$ $F = 4$ and $F = 3$ are close to each other, making it easier to achieve two-mode operation than the condition where one of the peak transmissions dominants. The full width at half maximum (FWHM) of FADOF transmittance spectrum corresponding to F = 4 and F = 3 are both around 1 GHz. Hence, there are around 4 cavity modes within one FWHM. In particular, only two laser modes $L_1$ and $L_2$ are observed, so only one laser mode survived within each FWHM. Besides, the frequency difference between $f_1$ and $f_2$ of DF Faraday laser is large enough, which is 7.43-8.80 GHz in this work, that is, there are at least 34 cavity modes between $L_1$ and $L_2$. Therefore, the mode competition between $L_1$ and $L_2$ has little impact on the frequency of each mode, which is covered in more detail in Section 3.4.

The two-mode operation is verified by studying the beat-note spectrum between the reference IF-ECDL and the DF Faraday laser. The power of IF-ECDL and DF Faraday laser for optical heterodyne are both 0.4 mW. The beat-note spectra between the reference laser and the DF Faraday laser at the vapor-cell temperature range of $36 - 55\,^{\circ}$C are shown in Fig. 3(a) with ordinate scale being linear in voltage. The beat-note spectra at different vapor-cell temperatures all have four beating components with central frequencies from low to high being $f_1 - f_0$, $f_2 - 2f_1 + f_0$, $f_2 - f_1$, and $f_2 - f_0$, respectively. Moreover, the four beating components, in the form of frequency, are the beat-note signals of $f_1 - f_0$ and $(f_2 - f_0) - (f_2 - f_1)$, $(f_2 - f_1) - (f_1 - f_0)$ and $((f_2 - f_0) - (f_1 - f_0)) - (f_1 - f_0)$, $f_2 - f_1$ and $(f_2 - f_0) - (f_1 - f_0)$, and $f_2 - f_0$, separately. The more distinct examples of the beat-note spectra in log scale are depicted in Fig. 3(b) and (c) at vapor-cell temperature of $38\,^{\circ}$C and $53\,^{\circ}$C, respectively.

The amplitude of each beating component with the variation of vapor-cell temperature is shown in Fig. 3(d). Due to the different constituents of each beating component, it is difficult to measure the laser powers of $L_1$ and $L_2$ based on the beat-note spectrum. Fig. 3(e) and (f) are two expanded beat-note spectra of Fig. 3(b) at frequencies $f_1 - f_0$ and $f_2 - f_0$ with Lorentz fitted linewidths being 30 kHz and 33 kHz, respectively. The difference between the two fitted linewidths is owing to the slightly power difference between $L_1$ and $L_2$, because the laser linewidth is inversely proportional to

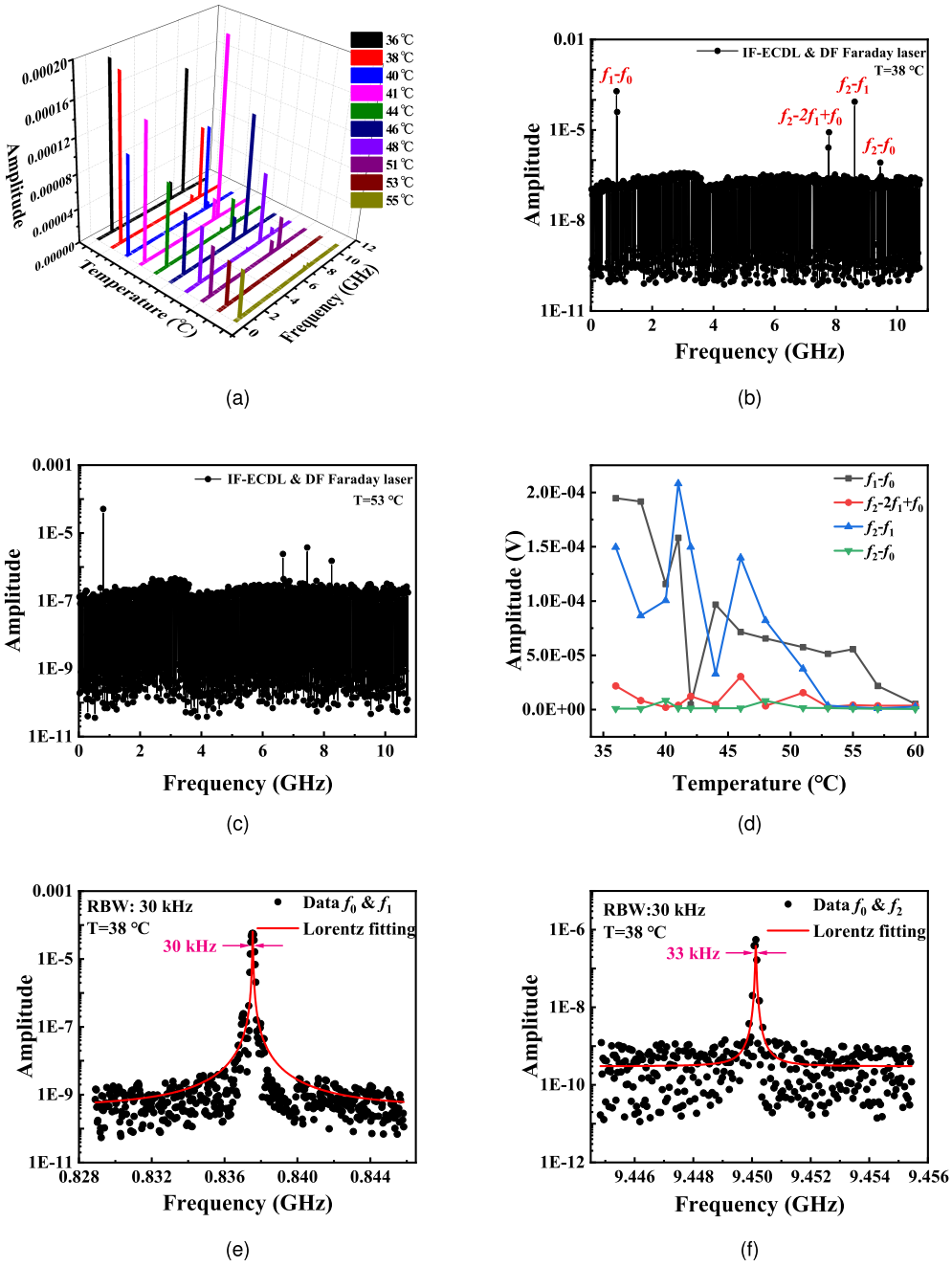


Fig. 3. (a) The beat-note spectra between reference IF-ECDL and DF Faraday laser at different vapor-cell temperatures. The spectra at each vapor-cell temperature are all composed of four beating components, but the fourth peak from low to high frequency is too weak to observe using a linear scale axis. (b) Beat-note spectrum of Fig. 3(a) at vapor-cell temperature of 38 °C in log scale. The central frequencies of the four beating components from left to right are $f_1 - f_0$, $f_2 - 2f_1 + f_0$, $f_2 - f_1$, and $f_2 - f_0$, respectively. (c) Beat-note spectrum of Fig. 3(a) at vapor-cell temperature of 53 °C in log scale. (d) The beating amplitudes corresponding to the four components of each beat-note spectrum in Fig. 3(a) as a function of vapor-cell temperature. (e) The expanded beat-note spectra in Fig. 3(b) at frequency $f_1 - f_0$ and (f) $f_2 - f_0$. The lorentz fitted linewidths are 30 kHz and 33 kHz, respectively, with resolution bandwidth being 30 kHz.

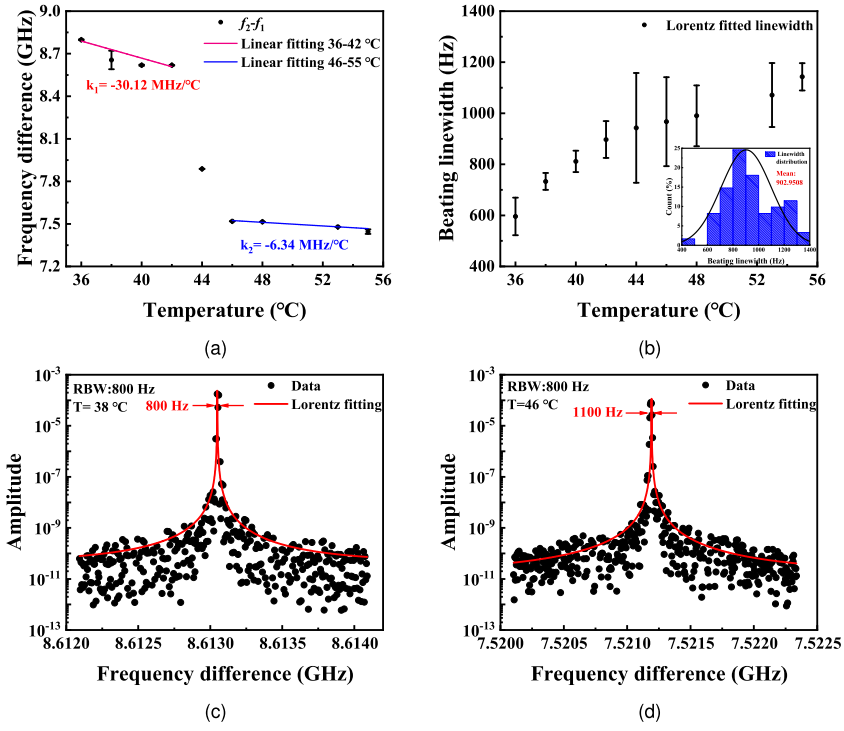


Fig. 4. (a) The frequency difference between $f_1$ and $f_2$ of DF Faraday laser as a function of vapor-cell temperature, where the red dash-dotted line represents the linear fitting of experimental data in the vapor-cell temperature range of 36–42 °C, and the blue dotted line is under 46–55 °C. The sharp variation of frequency difference in 42–46 °C results from mode hopping. (b) The Lorentz fitted linewidth of beat-note spectrum between the two modes $L_1$ and $L_2$ of DF Faraday laser as a function of the vapor-cell temperature. The insert represents the linewidth distribution of the beat-note spectra between the two modes at the vapor-cell temperature range of 36–55 °C with the most probable beating linewidth being 902.95 Hz. The data at each vapor-cell temperature in Fig. 4(a) and Fig. 4(b) is the result of 20 measurements in three days. (c) Experimental data of beat-note spectra between two modes $L_1$ and $L_2$ of DF Faraday laser at vapor-cell temperature of 38 °C and (d) 46 °C with fitted linewidths being 800 Hz and 1100 Hz, respectively. The resolution bandwidth are both 800 Hz.

the laser power [36]. Essentially, the power difference between $L_1$ and $L_2$ comes from the slightly difference between peak transmissions of the FADOF transmittance spectrum corresponding to $F = 4$ and $F = 3$.

### 3.3 The Beat-Note Spectrum Between the Two Modes of DF Faraday Laser

The frequency difference and beating linewidth between the two modes $L_1$ and $L_2$ as a function of vapor-cell temperature are depicted in Fig. 4(a) and (b), respectively. The experimental results at each temperature is measured 20 times in three days.

As shown in Fig. 4(a), the frequency difference $\Delta f$ between $f_1$ and $f_2$ of DF Faraday laser drops from 8.80 GHz to 7.43 GHz as the vapor-cell temperature $T$ rises from 36 °C to 55 °C (with step of 2 °C). The frequency-difference variation with the vapor-cell temperature, $d\Delta f/dT$, is related to the temperature range, therefore, it is analyzed with piecewise linear fitting. The value of $d\Delta f/dT$ is experimentally determined to be $-30.12 \pm 5.91$ MHz/°C ($-6.34 \pm 0.58$ MHz/°C) at temperature range of $36 - 42$ °C ($46 - 55$ °C), which is shown as the fitting slope $k_1$ ($k_2$) in Fig. 4(a). The variation of frequency difference $\Delta f$ with vapor-cell temperature $T$ is principally the result of two causes: Firstly, the cavity length of DF Faraday laser changes with $T$, and leads to the change of cavity-mode frequency. Secondly, the transmittance spectrum of FADOF is a function of $T$, hence, the temperature influences the peak transmission frequencies of FADOF transmittance spectrum.

The cylindrical atomic vapor cell inside the FADOF is 30 mm long with wall-thickness being 1 mm at both sides, and the cavity length of the DF Faraday laser is 69 cm. The thermal expansion coefficient $\alpha$ and the refractive index $n$ of the glass vapor cell are respectively $8 \times 10^{-6}$/°C and 1.55, thus, the variation ratio of cavity length with vapor-cell temperature is $-24.18$ nm/°C. Considering that the FSR of DF Faraday laser is 217 MHz, the change of cavity-mode frequency with vapor-cell temperature, $df/dT$, is $-12.32$ MHz/°C.

If we only take impact of cavity-mode frequency on the frequencies of the two modes into account, $d\Delta f/dT$ can be ignored when the two frequencies $f_1$ and $f_2$ drift in one direction with the cavity-mode frequency. Conversely, $d\Delta f/dT$ is twice as much as the $df/dT$, namely, around $-24.64$ MHz/°C. Fig. 4(a) shows that the two frequencies $f_1$ and $f_2$ of DF Faraday laser shift in opposite direction at the vapor-cell temperature range of 36–42 °C, and in the same direction at 46–55 °C. The fitting slopes $k_1$ and $k_2$ are not exactly the same as the theoretical results, since the two frequencies $f_1$ and $f_2$ depend not only on the cavity-mode frequency, but also on the transmittance spectrum of FADOF corresponding to $F = 4$ and $F = 3$. Accordingly, the linear fitting values of experimental data, $k_1$ and $k_2$, are about 6 MHz/°C different from the theoretical values. The sharp change of $\Delta f$ between 42–46 °C comes form the mode hopping. Nevertheless, the frequency interval between $f_1$ and $f_2$ is tunable via adjusting the vapor-cell temperature.

Because the FWHM of FADOF transmission spectrum and the FSR are around 1 GHz and 217 MHz, respectively, and the resonance bandwidth of the cavity mode $\Delta\nu_c$ is much smaller than the FWHM, the frequencies $f_1$ and $f_2$ of DF Faraday laser can not exactly coincide with the peak frequencies of FADOF transmittance spectrum corresponding to $F = 4$ and $F = 3$. Therefore, the frequency interval between $f_1$ and $f_2$ is not exactly equal to the hyperfine energy interval of Cs ground state, 9.19 GHz. This shortcoming can be overcome by adjusting the cavity length of DF Faraday laser so that 9.19 GHz is an exact integral multiple of the FSR. In addition, the frequency of Faraday laser is confined to the narrow transmission bandwidth of FADOF, which is immune to the fluctuations of temperature and current of LD [16]. Moreover, the frequency difference between the two modes is immune to the cavity-length fluctuation under appropriate vapor-cell temperature range (36–42 °C in this work).

The beating linewidths between the two modes $L_1$ and $L_2$ at different vapor-cell temperatures are measured, as shown in Fig. 4(b). The insert represents the linewidth distribution of the beat-note spectra between the two generated laser modes at the vapor-cell temperature range of 36–55 °C with the most probable beating linewidth being 902.95 Hz. Although without mode locking, the experimental results indicate that the coherence between the two modes is good. This is due to the two modes sharing one cavity, so the common mode noise caused by the change of cavity length, vapor-cell temperature, magnetic field and the temperature and current of the laser diode is greatly suppressed. Therefore, the beating linewidth of the two laser modes is much narrower than the linewidth of each laser mode. Fig. 4(c) and (d) are two examples of the beating spectrum of the two modes at vapor-cell temperature of 38 °C and 46 °C, with Lorentz fitted linewidths being 800 Hz and 1100 Hz, separately.

As shown in Fig. 4(b), the beating linewidth is broadened as vapor-cell temperature increased, because that the FWHMs of FADOF transmittance spectrum corresponding to $F = 4$ and $F = 3$ are both increased with the rise of temperature, which will lead to a stronger competition between the modes inside one passband of FADOF transmittance spectrum. Next, we will analyze the mode competition in one passband of FADOF transmittance spectrum, and that in two separate passbands in detail.

### 3.4 Mode Competion

By measuring the beat-note spectrum between the two modes $L_1$ and $L_2$ of the DF Faraday laser, we only observe one beating component, whose central frequency is in the range of 7.43–8.80 GHz under the change of vapor-cell temperature, and there is no other beating component with frequency interval being the mode spacing of 217 MHz. Experiments show that, although there are around 4 cavity modes within the FWHM of one passband of FADOF transmittance spectrum,

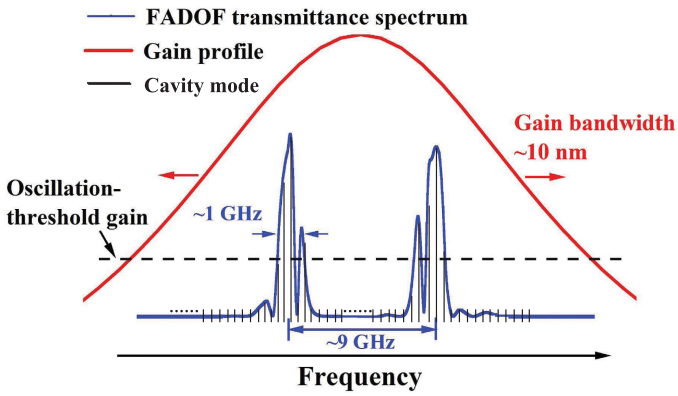


Fig. 5. Two simultaneously oscillating modes in the DF Faraday laser. The red curve is the semiconductor gain with bandwidth of around 10 nm, and the blue curve represents the two separate passbands of FADOF transmittance spectrum corresponding to F = 4 and F = 3, and the FWHM of each passband is around 1 GHz. The black lines indicate the cavity modes with mode spacing of 217 MHz.

only the cavity mode whose center frequency is closest to the peak transmission frequency of each passband can survive.

Essentially, the proposed DF Faraday laser is a type of the ECDL, which has the characteristic of homogeneously broadening. For the typical ECDLs, by putting the mode-selection elements, for instance, IFs [21], [22], gratings [23], [24], or Fabry-Pérot etalons [25], [26], inside the external cavity, the frequency of the survived single longitude mode from ECDLs can be controlled in the range of several tens of GHz within the diode gain bandwidth of about 10 nm. As a comparison, the Faraday laser has a narrow-bandwidth feature since the narrow-bandwidth atomic filter is used as the frequency-selection element placed in the external cavity of semiconductor laser. Owing to the anomalous Faraday effect, only the laser mode with frequency in the transmission bandwidth of FADOF can be transmitted, which ensures that the output laser frequency is controlled in the range of several GHz or even MHz [3].

For clarity, we present a sketch of FADOF transmittance spectrum in the semiconductor gain bandwidth of DF Faraday laser, as shown in Fig. 5. Since the semiconductor gain bandwidth is around 10 nm, and the mode spacing is 217 MHz, there are actually thousands of cavity modes within the gain bandwidth. However, after mode selection by FADOF whose FWHM of each passband is about GHz, only around 4 modes can be possibly output.

Suppose that the gain of the 4 modes are all higher than the threshold gain of oscillation, and the mode competition in the two passbands of FADOF transmittance spectrum is considered separately. The laser mode that survived in each passband is regarded as a homogeneously broadened laser, like the common semiconductor laser, where several modes satisfying the threshold gain condition compete with each other in the process of oscillation, ultimately, only the mode close to the center frequency survived and oscillate stably, while the other modes are suppressed and extinguished [37]. Consequently, only one mode can be output in each passband of FADOF transmittance spectrum.

It should note that, here, we assume that the mode competition in two passbands of FADOF transmittance spectrum are almost independent. However, there is still competition between the two modes $L_1$ and $L_2$ output from the respective passband. One reason of this assumption is that, in our experiment, by changing the vapor-cell temperature, the frequency difference between the two modes is changed within the interval 7.43–8.80 GHz, which means there are at least 34 cavity modes between the two output modes, thus the competition between $L_1$ and $L_2$ is weak. Moreover, by adjusting the current and temperature of LD, magnetic field, and the vapor-cell temperature, the transmissions of the transmittance spectra corresponding to F = 4 and F = 3 are nearly equal, so that the difference between the gain of two modes is not significant. Hence, both modes

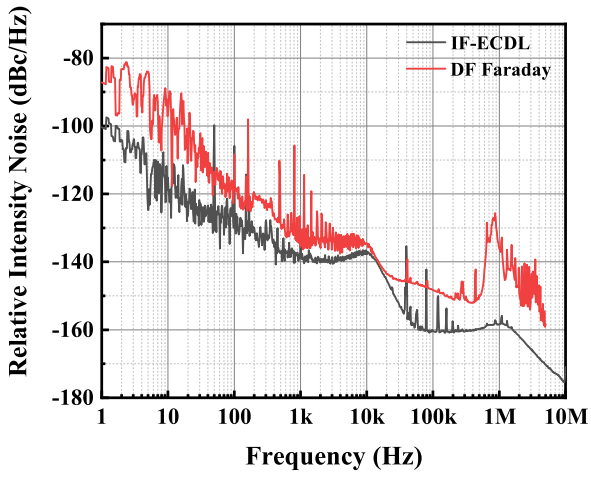


Fig. 6. The measured relative intensity noise of the 852 nm DF Faraday laser (red curve) and the homemade 852 nm IF-ECDL (black curve).

can oscillate simultaneously in each passband of FADOF transmittance spectrum with each mode oscillating almost independent of the other mode.

To evaluate the impact of mode competition between $L_1$ and $L_2$ on the optical power intensity, we measured the relative intensity noise (RIN) of the DF Faraday laser. For comparison, the RIN of the homemade 852 nm IF-ECDL shown in Fig. 1, is also measured. The optical signals of the DF Faraday laser and the IF-ECDL are converted to electric signals by the photodiode, then the intensity noises of the electric signals are separately measured by a signal source analyzer (Keysight E5052B). As depicted in Fig. 6, with the tested frequency range from 1 Hz to 10 MHz, the RIN measurement results of the DF Faraday laser and the IF-ECDL are shown by the red and black curves. It demonstrates that the RIN of the DF Faraday laser is worse than the IF-ECDL, especially at the frequency above 10 kHz. The RIN performances of the DF Faraday laser and the IF-ECDL are measured to be $-134$ dBc/Hz and $-137$ dBc/Hz at 10 kHz offset when the optical power entering the photodiode are both 1 mW.

Although the competition between the two modes is weak, it will partly affect the RIN of the laser. However, the two modes are difficult to be separated at present, hence, the RIN of each laser mode is not analyzed. Since it is important to measure the RIN of each mode to further improve the performance of DF Faraday laser, we will measure and optimize the RIN of each laser mode in our next works.

### *3.5 Applications*

Experiments show that the DF Faraday laser has many merits compared with other two-mode lasers. For instance, the two frequencies $f_1$ and $f_2$ of DF Faraday laser are tied to the atomic transition frequencies, and therefore intrinsically stable. In addition, the frequency interval between the two modes $L_1$ and $L_2$ of DF Faraday laser is adjustable with the vapor-cell temperature, which can be analogy to the DF Tm:YAG laser [28]. Further, $L_1$ and $L_2$ have excellent coherence with linewidth being tens of kHz of each laser mode.

Here we present four potential applications of Faraday laser in atomic physics. Firstly, the DF Faraday laser is a favorable light source for the development of high-contrast Doppler-free spectroscopy. Utilizing DF laser field, the fractional frequency stability of diode laser can be improved by about one order of magnitude compared to the traditional single-frequency SAS [29], [30]. Secondly, through carefully designing the cavity length of DF Faraday laser, the integer number of FSR can be exactly equal to the hyperfine frequency interval of Cs ground state, such a DF Faraday

laser can be used as the coherent light source for CPT atomic clocks [31], [32], [38]. Thirdly, the DF Faraday laser, with potential in transmitting signal from optical domain to microwave domain like the frequency comb, will infuse new elements to optical generation microwave field. Finally, analogous to the frequency stabilization of two-mode He-Ne laser [27], the coherence between the two laser modes can be further enhanced by locking the frequency interval between the two modes of DF Faraday laser to a reference laser (Cs atomic clock) through phase locking technique [39], [40]. With feedback error signal to the piezoelectric transduce connected with the external-cavity mirror to lock the cavity length, the linewidth of each laser mode is expected to be further narrowed.

## 4. Conclusion

In conclusion, we demonstrate a novel DF Faraday laser with two simultaneous output modes. The central frequencies of the two modes mainly depend on the peak transition frequencies of FADOF transmittance spectrum corresponding to $F = 4$ and $F = 3$, respectively. The laser linewidth of each laser mode is narrower than 33 kHz, and the most probable linewidth of the beat-note spectra between the two modes is 902.95 Hz at different vapor-cell temperatures. The frequency difference between the two modes is tunable over a range of 1.4 GHz, and the tuning is realized via adjusting the temperature of the Cs vapor cell in the FADOF. Such a DF Faraday laser has potential applications in the experiments of Doppler-free spectroscopy and CPT atomic clocks. Additionally, this system can be extended to other atoms. For instance, we experimentally verified that the 780 nm Rb Faraday laser also has DF characteristic with frequency interval between the two modes being tunable from 5.1 GHz to 6.2 GHz.

## References


[1] B. Yin and T. Shay, "Theoretical model for a Faraday anomalous dispersion optical filter," *Opt. Lett.*, vol. 16, no. 20, pp. 1617–1619, 1991.

[2] M. A. Zentile, J. Keaveney, R. S. Mathew, D. J. Whiting, C. S. Adams, and I. G. Hughes, "Optimization of atomic Faraday filters in the presence of homogeneous line broadening," *J. Phys. B: At., Mol. Opt. Phys.*, vol. 48, no. 18, 2015, Art. no. 185001.

[3] Y. Wang, S. Zhang, D. Wang, Z. Tao, Y. Hong, and J. Chen, "Nonlinear optical filter with ultranarrow bandwidth approaching the natural linewidth," *Opt. Lett.*, vol. 37, no. 19, pp. 4059–4061, 2012.

[4] M. A. Zentile, D. J. Whiting, J. Keaveney, C. S. Adams, and I. G. Hughes, "Atomic Faraday filter with equivalent noise bandwidth less than 1 GHz," *Opt. Lett.*, vol. 40, no. 9, pp. 2000–2003, 2015.

[5] S. D. Harrell *et al.*, "Sodium and potassium vapor Faraday filters revisited: Theory and applications," *J. Opt. Soc. America B*, vol. 26, no. 4, pp. 659–670, 2009.

[6] D. J. Dick and T. M. Shay, "Ultrahigh–noise rejection optical filter," *Opt. Lett.*, vol. 16, no. 11, pp. 867–869, 1991.

[7] E. T. Dressler, A. E. Laux, and R. I. Billmers, "Theory and experiment for the anomalous Faraday effect in potassium," *J. Opt. Soc. America B*, vol. 13, no. 9, pp. 1849–1858, 1996.

[8] Y. Zhang, X. Jia, Z. Ma, and Q. Wang, "Optical filtering characteristic of potassium Faraday optical filter," *IEEE J. Quantum Electron.*, vol. 37, no. 3, pp. 372–375, Mar. 2001.

[9] P. Yeh, "Dispersive magnetooptic filters," *Appl. Opt.*, vol. 21, no. 11, pp. 2069–2075, 1982.

[10] B. Yin and T. M. Shay, "Faraday anomalous dispersion optical filter for the Cs 455 nm transition," *IEEE Photon. Technol. Lett.*, vol. 4, no. 5, pp. 488–490, May 1992.

[11] Y. Ohman, "On some new auxiliary instruments in astrophysical research VI. A tentative monochromator for solar work based on the principle of selective magnetic rotation," *Stockholms Obs. Ann*, vol. 19, no. 4, pp. 9–11, 1956.

[12] H. Chen, M. White, D. A. Krueger, and C. She, "Daytime mesopause temperature measurements with a sodium-vapor dispersive Faraday filter in a lidar receiver," *Opt. Lett.*, vol. 21, no. 15, pp. 1093–1095, 1996.

[13] J. Höffner and C. Fricke-Begemann, "Accurate lidar temperatures with narrowband filters," *Opt. Lett.*, vol. 30, no. 8, pp. 890–892, 2005.

[14] P. Wanninger and E. Valdez, "Diode-laser frequency stabilization based on the resonant Faraday effect," *IEEE Photon. Technol. Lett.*, vol. 4, no. 1, pp. 94–96, Jan. 1992.

[15] K. Choi, J. Menders, P. Searcy, and E. Korevaar, "Optical feedback locking of a diode laser using a cesium Faraday filter," *Opt. Commun.*, vol. 96, no. 4-6, pp. 240–244, 1993.

[16] X. Miao *et al.*, "Note: Demonstration of an external-cavity diode laser system immune to current and temperature fluctuations," *Rev. Scientific Instrum.*, vol. 82, no. 8, 2011, Art. no. 086106.

[17] Z. Tao, X. Zhang, D. Pan, M. Chen, C. Zhu, and J. Chen, "Faraday laser using 1.2 km fiber as an extended cavity," *J. Phys. B: At., Mol. Opt. Phys.*, vol. 49, no. 13, 2016, Art. no. 13LT01.

[18] J. Keaveney, W. J. Hamlyn, C. S. Adams, and I. G. Hughes, "A single-mode external cavity diode laser using an intra-cavity atomic faraday filter with short-term linewidth $<$400 kHz and long-term stability of $<$1 MHz," *Rev. Scientific Instrum.*, vol. 87, no. 9, 2016, Art. no. 095111.

[19] P. Chang *et al.*, "A Faraday laser lasing on Rb 1529 nm transition," *Scientific Rep.*, vol. 7, 2017, Art. no. 8995.
[20] P. Chang *et al.*, "A Faraday laser operating on Cs 852 nm transition," *Appl. Phys. B*, vol. 125, no. 12, 2019, Art. no. 230.
[21] X. Baillard *et al.*, "Interference-filter-stabilized external-cavity diode lasers," *Opt. Commun.*, vol. 266, no. 2, pp. 609–613, 2006.
[22] M. Gilowski *et al.*, "Narrow bandwidth interference filter-stabilized diode laser systems for the manipulation of neutral atoms," *Opt. Commun.*, vol. 280, no. 2, pp. 443–447, 2007.
[23] K. Liu and M. G. Littman, "Novel geometry for single-mode scanning of tunable lasers," *Opt. Lett.*, vol. 6, no. 3, pp. 117–118, 1981.
[24] L. Ricci *et al.*, "A compact grating-stabilized diode laser system for atomic physics," *Opt. Commun.*, vol. 117, no. 5, pp. 541–549, 1995.
[25] H. Deok Kim, S.-G. Kang, and C.-H. Le, "A low-cost WDM source with an ASE injected Fabry-Perot semiconductor laser," *IEEE Photon. Technol. Lett.*, vol. 12, no. 8, pp. 1067–1069, Aug. 2000.
[26] Y. Zhao *et al.*, "100-Hz linewidth diode laser with external optical feedback," *IEEE Photon. Technol. Lett.*, vol. 24, no. 20, pp. 1795–1798, Oct. 2012.
[27] S. Yokoyama, T. Araki, and N. Suzuki, "Intermode beat stabilized laser with frequency pulling," *Appl. Opt.*, vol. 33, no. 3, pp. 358–363, 1994.
[28] G. Quehl, J. Grünert, V. Elman, and A. Hemmerich, "A tunable dual frequency Tm:YAG laser," *Opt. Commun.*, vol. 190, no. 1-6, pp. 303–307, 2001.
[29] M. A. Hafiz, G. Coget, E. De Clercq, and R. Boudot, "Doppler-free spectroscopy on the Cs D1 line with a dual-frequency laser," *Opt. Lett.*, vol. 41, no. 13, pp. 2982–2985, 2016.
[30] M. A. Hafiz *et al.*, "High-contrast sub-Doppler absorption spikes in a hot atomic vapor cell exposed to a dual-frequency laser field," *New J. Phys.*, vol. 19, no. 7, 2017, Art. no. 073028.
[31] E. Arimondo, "V coherent population trapping in laser spectroscopy," in *Prog. Opt.*, vol. 35. New York, NY, USA: Elsevier, 1996, pp. 257–354.
[32] K. Bergmann, H. Theuer, and B. Shore, "Coherent population transfer among quantum states of atoms and molecules," *Rev. Mod. Phys.*, vol. 70, no. 3, pp. 1003–1025, 1998.
[33] D. A. Steck, "Cesium D line data," 2003. [Online]. Available: http://steck.us/alkalidata
[34] B. Luo, L. Yin, J. Xiong, J. Chen, and H. Guo, "Signal intensity influences on the atomic Faraday filter," *Opt. Lett.*, vol. 43, no. 11, pp. 2458–2461, 2018.
[35] J. Keaveney, C. S. Adams, and I. G. Hughes, "Elecsus: Extension to arbitrary geometry magneto-optics," *Comput. Phys. Commun.*, vol. 224, pp. 311–324, 2018.
[36] A. L. Schawlow and C. H. Townes, "Infrared and optical masers," *Phys. Rev.*, vol. 112, no. 6, pp. 1940–1949, 1958.
[37] A. E. Siegman, *Lasers*. Mill Valley, CA, USA: University Science, 1986.
[38] M. A. Hafiz *et al.*, "Toward a high-stability coherent population trapping Cs vapor-cell atomic clock using autobalanced Ramsey spectroscopy," *Phys. Rev. Appl.*, vol. 9, no. 6, 2018, Art. no. 064002.
[39] G. Santarelli, A. Clairon, S. Lea, and G. Tino, "Heterodyne optical phase-locking of extended-cavity semiconductor lasers at 9 GHz," *Opt. Commun.*, vol. 104, nos. 4–6, pp. 339–344, 1994.
[40] T. Shi, D. Pan, and J. Chen, "Realization of phase locking in good-bad-cavity active optical clock," *Opt. Express*, vol. 27, no. 16, pp. 22 040–22 052, 2019.